30 August 2005

On the Modeling of Step-and-Flash Imprint Lithography using Molecular Statics Models

Maciej Paszynski [a 1], Albert Romkes [a], Elizabeth Collister [b], Jason Meiring [b], Leszek F. Demkowicz [a], and C. Grant Willson [b]

[a] *Institute for Computational Engineering and Sciences*
The University of Texas at Austin
Austin, Texas 78712

[b] *Department of Chemical Engineering*
The University of Texas at Austin
Austin, Texas 78712

Abstract

We introduce linear and nonlinear molecular statics models for the prediction of the material response of polymerized networks in cured etch-barrier layers that are formed during the so-called Step-and-Flash Imprint Lithography (SFIL) process. The molecular structure of the polymerized network is obtained via a Monte-Carlo simulation of the chemical reactions that take place during the curing of the etch-barrier layer. The resulting molecular structure consists of a lattice of point mass particles with pairwise, nearest-neighbor, force interactions governed by potentials. We introduce three molecular statics models: (1) A linear model assuming small deformations and inter-molecular bonds governed by quadratic force potential functions. (2) A non-linear model allowing for large deformations, still with quadratic force potential functions. (3) A non-linear model allowing for large deformations and assuming non-linear Lennard-Jones potential functions. We demonstrate the application of these molecular models by showing numerical results on the deformation of a small-size (50×50×50 nm) representative feature in common etch-barrier layers. These molecular statics models simulations are compared to the results obtained by finite element approximations of a linear elasticity model in which the shrinkage of the feature is enforced by the thermal expansion coefficient (CTE).

[1] On leave from *AGH University of Science and Technology, Department of Computer Methods in Metallurgy, Cracow, Poland*, e-mail: maciek@ices.utexas.edu

1 Introduction

Step and flash imprint lithography (SFIL) is a patterning process utilizing photopolymerization to replicate the topography of a template onto a substrate [2,3].

The major processing steps of SFIL include: depositing a low viscosity, silicon-containing, photocurable etch barrier on to a substrate; bringing the template into contact with the etch barrier; curing the etch barrier solution through UV exposure; releasing the template, while leaving high-resolution features behind; a short, halogen break-through etch; and finally an anisotropic oxygen reactive ion etch to yield high aspect ratio, high resolution features.

Photopolymerization, however, is often accompanied by densification. The interaction potential between photopolymer precursors undergoing free radical polymerization changes from van der Waals' to covalent. The average distance between molecules decreases and causes volumetric contraction. Densification of the SFIL photopolymer (the etch barrier) may affect both the cross sectional shape of the feature and the placement of relief patterns.

The Monte-Carlo algorithm for the simulation of the chemical reactions that take place during the curing of the etch-barrier layer [6] together with the molecular statics models make it possible to explore the influence of densification and mechanical properties on changes in the placement and in the geometry of the replicated features.

We introduce linear and non-linear molecular statics models for the prediction of the material response of polymerized networks in cured etch-barrier layers that are formed during the so-called Step-and-Flash Imprint Lithography (SFIL) process. To obtain physically reasonable realizations of such networks, a Monte-Carlo algorithm for the simulation of the chemical reactions that take place during the curing of the etch-barrier layer was developed [6]. The resulting molecular structure consists of a lattice of point mass particles with pairwise, nearest-neighbor, force interactions governed by force potential functions. In the linear molecular statics model, particle displacements are assumed to remain small and all inter-molecular bonds are governed by quadratic force potential functions. We additionally introduce nonlinear models that allow for large particle displacements and may employ Lennard-Jones type potential functions to prescribe the non-covalent force interactions. We demonstrate the application of these molecular models by showing numerical results on the deformation of a small-size ($50\times50\times50$ nm) representative

feature in common etch-barrier layers.

We compare the molecular statics models with linear elasticity model approximated by the finite element method, where the shrinkage of the feature is enforced by the thermal expansion coefficient (CTE).

2 The SFIL Process

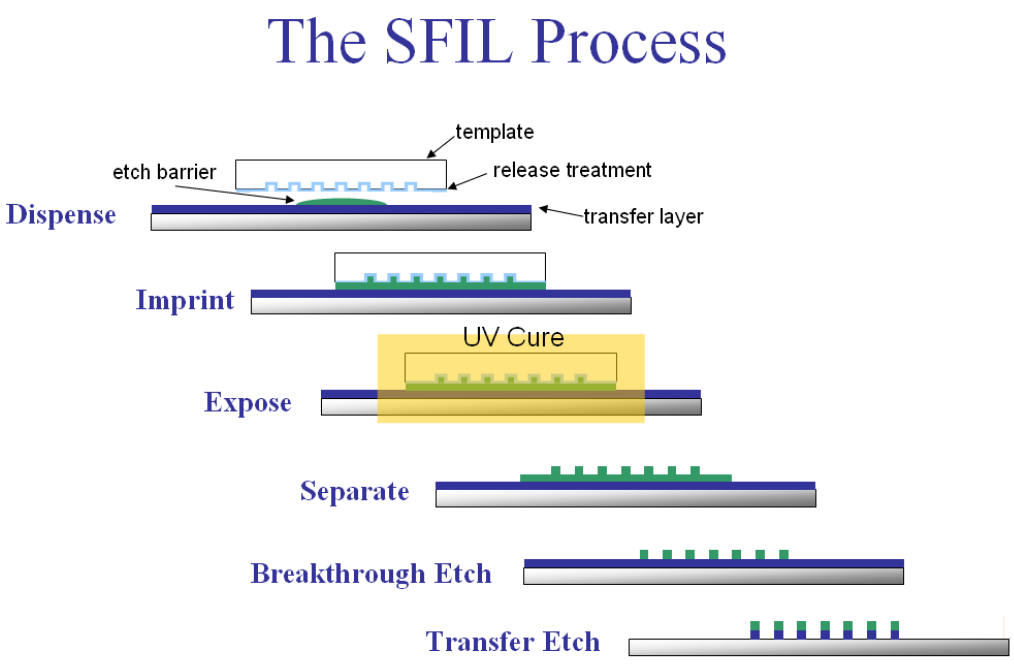

Fig. 2.1: SFIL process.

The SFIL process can be described in the following steps, according to [3].

- *Dispense*. The SFIL process employs a template / substrate alignment scheme to bring a rigid template and substrate into parallelism, trapping the etch barrier in the relief structure of the template.
- *Imprint*. The gap is closed until the force that ensures a thin base layer is reached.
- *Exposure*. The template is then illuminated through the backside to cure etch barrier.
- *Separate*. The template is withdrawn, leaving low-aspect ratio, high resolution features in the etch barrier.
- *Breakthrough Etch*. The residual etch barrier (base layer) is etched away with a short halogen plasma etch.
- *Transfer Etch* The pattern is transferred into the transfer layer with an anisotropic oxygen reactive ion etch, creating high-aspect ratio, high resolution features in the organic transfer layer.

3 Modeling of the Cured Etch Barrier

A Monte Carlo method is used to simulate the chemical reaction processes that occur during the photo-curing of the etch barrier. The algorithm produces the molecular structure of the polymerized etch barrier in the form of a lattice structure of molecules with connecting springs representing the intermolecular covalent or *van der Waals* bonds. A comprehensive description of this algorithm is given in [6]. To predict the deformation of the obtained lattice structure, we derive linear and nonlinear molecular statics models, described in the following sections.

3.1 The Molecular Statics Models

In the following, we derive a general equation governing the equilibrium configurations of the molecular lattice structures that are produced by the Monte Carlo simulation of the photo-curing process.

In Figure 3.1, we consider an arbitrary pair of bonded molecules in the lattice with indices α and β which have the lattice position vectors $\mathbf{p}_\alpha = (\hat{x}_\alpha, \hat{y}_\alpha, \hat{z}_\alpha)$ and $\mathbf{p}_\beta$. The unknown equilibrium position vectors of particles α and β, under the action of all their intermolecular bonds, are denoted $\mathbf{x}_\alpha = (x_\alpha, y_\alpha, z_\alpha)$ and $\mathbf{x}_\beta$, respectively (see Figure 3.1). In addition, the displacements from the initial position in the lattice to the equilibrium position are represented by the vectors $\mathbf{u}_\alpha = \mathbf{x}_\alpha - \mathbf{p}_\alpha$ and $\mathbf{u}_\beta = \mathbf{x}_\beta - \mathbf{p}_\beta$. Let $\|\cdot\|$ denote the Euclidean norms in $\mathbb{R}^3$ and let $r_{\alpha\beta} = \|\mathbf{x}_\beta - \mathbf{x}_\alpha\|$ be the distance between particles α and β in initial configuration. Then, the force $\mathbf{F}_{\alpha\beta}$, along the vector $\mathbf{x}_\beta - \mathbf{x}_\alpha$, that is acting on the particle α due to the bond between particles α and β is governed by the potential function $V(r_{\alpha\beta})$,

$$\mathbf{F}_{\alpha\beta} = -\underbrace{\frac{\partial V(r_{\alpha\beta})}{\partial r_{\alpha\beta}}}_{\text{magnitude}} \underbrace{\frac{\mathbf{x}_\beta - \mathbf{x}_\alpha}{\|\mathbf{x}_\beta - \mathbf{x}_\alpha\|}}_{\text{direction}} \tag{1}$$

If the indices of bonded neighboring particles of particle α are collected in the set $\mathcal{N}_\alpha$, then we obtain its force equilibrium by applying the following sum:

$$\sum_{\beta \in \mathcal{N}_\alpha} \mathbf{F}_{\alpha\beta} = -\sum_{\beta \in \mathcal{N}_\alpha} \frac{\partial V(r_{\alpha\beta})}{\partial r_{\alpha\beta}} \frac{\mathbf{x}_\beta - \mathbf{x}_\alpha}{\|\mathbf{x}_\beta - \mathbf{x}_\alpha\|} = \mathbf{0}. \tag{2}$$

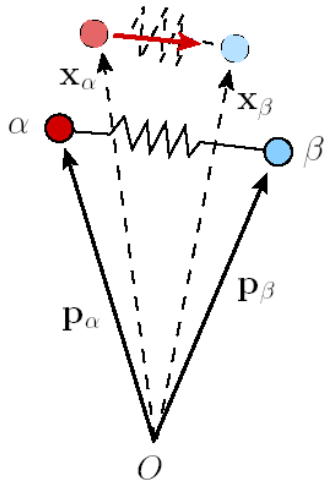

Fig. 3.1: Bonded pair of molecules.

The characteristics of the potential functions $\{V(r_{\alpha\beta})\}_{\beta\in\mathcal{N}_\alpha}$ are provided by the Monte Carlo simulation algorithm discussed in [6] and determine the character of the bonds, *i.e.* whether they are covalent or *van der Waals* bonds. Based on different assumptions on the force potential functions and the degree of deformation, we derive one linear and two nonlinear Molecular Statics models from (2) that govern the equilibrium positions $\{\mathbf{x}_\alpha\}$ of the particles in the deformed polymerized network.

3.1.1 Linear Model

The linear Molecular Statics model is based on two basic assumptions:

(1) All the force potential functions $V(r_{\alpha\beta})$ are quadratic and therefore the magnitude of the intermolecular forces $\mathbf{F}_{\alpha\beta}$ is linearly dependent on $r_{\alpha\beta}$, *i.e.* (1) becomes
$$F_{\alpha\beta} = k_{\alpha\beta}\left(r_{\alpha\beta} + \Delta r_{\alpha\beta} - r^0_{\alpha\beta}\right)$$
where $r_{\alpha\beta} + \Delta r_{\alpha\beta}$ is length of the spring in equillibrium configuration of the lattice structure and $r^0_{\alpha\beta}$ is the unstretched length of the spring (when $\mathbf{F}_{\alpha\beta} = \mathbf{0}$).

(2) Small deformations are assumed. So that the direction of the spring forces is aligned with the initial vectors $\mathbf{p}_\beta - \mathbf{p}_\alpha$.

In the initial configuration, the spring is aligned along $\mathbf{p}_\alpha - \mathbf{p}_\beta$. In the equilibrium configuration it is aligned along $\mathbf{x}_\beta - \mathbf{x}_\alpha$. The angle between these two alignments is governed by
$$\cos\theta = \frac{(\mathbf{p}_\beta - \mathbf{p}_\alpha)\cdot(\mathbf{x}_\beta - \mathbf{x}_\alpha)}{\|\mathbf{p}_\beta - \mathbf{p}_\alpha\|\|\mathbf{x}_\beta - \mathbf{x}_\alpha\|} = \frac{(\mathbf{p}_\beta - \mathbf{p}_\alpha)\cdot(\mathbf{x}_\beta - \mathbf{x}_\alpha)}{r_{\alpha\beta}\cdot(r_{\alpha\beta} + \Delta r_{\alpha\beta})}$$

Since we assumed small deformations

$$1 \approx \frac{(\mathbf{p}_\beta - \mathbf{p}_\alpha) \cdot (\mathbf{x}_\beta - \mathbf{x}_\alpha)}{r_{\alpha\beta} \cdot (r_{\alpha\beta} + \Delta r_{\alpha\beta})}$$

we get

$$r_{\alpha\beta} + \Delta r_{\alpha\beta} \approx \frac{1}{r_{\alpha\beta}} (\mathbf{p}_\beta - \mathbf{p}_\alpha) \cdot (\mathbf{x}_\beta - \mathbf{x}_\alpha)$$

The magnitude of the force in the spring between particles α and β becomes now

$$F_{\alpha\beta} = k_{\alpha\beta}(r_{\alpha\beta} + \Delta r_{\alpha\beta} - r^0_{\alpha\beta}) = \frac{k_{\alpha\beta}}{r_{\alpha\beta}} (\mathbf{p}_\beta - \mathbf{p}_\alpha) \cdot (\mathbf{x}_\beta - \mathbf{x}_\alpha) - k_{\alpha\beta} r^0_{\alpha\beta}$$

The force vector $\mathbf{F}_{\alpha\beta}$ is approximately aligned along $\mathbf{p}_\beta - \mathbf{p}_\alpha$, i.e.

$$\mathbf{F}_{\alpha\beta} = [\frac{k_{\alpha\beta}}{r_{\alpha\beta}} (\mathbf{p}_\beta - \mathbf{p}_\alpha) \cdot (\mathbf{x}_\beta - \mathbf{x}_\alpha) - k_{\alpha\beta} r^0_{\alpha\beta}] \frac{(\mathbf{p}_\beta - \mathbf{p}_\alpha)}{r_{\alpha\beta}}$$

where $[\frac{k_{\alpha\beta}}{r_{\alpha\beta}} (\mathbf{p}_\beta - \mathbf{p}_\alpha) \cdot (\mathbf{x}_\beta - \mathbf{x}_\alpha) - k_{\alpha\beta} r^0_{\alpha\beta}]$ represents the magnitude and $\frac{(\mathbf{p}_\beta - \mathbf{p}_\alpha)}{r_{\alpha\beta}}$ the direction of the force.

Equilibrium equations for linear model

At each particle, force equilibrium has to hold. Thus

$$\sum_\beta \mathbf{F}_{\alpha\beta} = \mathbf{0}, \quad \alpha = 1, 2, ..., N$$

which can be rewritten as

$$\sum_\beta (\frac{k_{\alpha\beta}}{r_{\alpha\beta}} (\mathbf{p}_\beta - \mathbf{p}_\alpha) \cdot (\mathbf{x}_\beta - \mathbf{x}_\alpha)) \frac{\mathbf{p}_\beta - \mathbf{p}_\alpha}{r_{\alpha\beta}} = \sum_\beta \frac{k_{\alpha\beta} r^0_{\alpha\beta}}{r_{\alpha\beta}} (\mathbf{p}_\beta - \mathbf{p}_\alpha) = \mathbf{0}$$

Note that $r_{\alpha\beta} = \sqrt{(\hat{x}_\beta - \hat{x}_\alpha)^2 + (\hat{y}_\beta - \hat{y}_\alpha)^2 + (\hat{z}_\beta - \hat{z}_\alpha)^2}$. So at each particle we have 3 equations (corresponding to each component of the vector equation).

For example, equations in x direction

$$\sum_\beta \frac{k_{\alpha\beta}[(\hat{x}_\beta - \hat{x}_\alpha)(x_\beta - x_\alpha) + (\hat{y}_\beta - \hat{y}_\alpha)(y_\beta - y_\alpha) + (\hat{z}_\beta - \hat{z}_\alpha)(z_\beta - z_\alpha)](\hat{x}_\beta - \hat{x}_\alpha)}{(\hat{x}_\beta - \hat{x}_\alpha)^2 + (\hat{y}_\beta - \hat{y}_\alpha)^2 + (\hat{z}_\beta - \hat{z}_\alpha)^2} =$$

$$\sum_\beta \frac{k_{\alpha\beta} r^0_{\alpha\beta} (\hat{x}_\beta - \hat{x}_\alpha)}{\sqrt{(\hat{x}_\beta - \hat{x}_\alpha)^2 + (\hat{y}_\beta - \hat{y}_\alpha)^2 + (\hat{z}_\beta - \hat{z}_\alpha)^2}}$$

equations in y direction

$$\sum_\beta \frac{k_{\alpha\beta}[(\hat{x}_\beta - \hat{x}_\alpha)(x_\beta - x_\alpha) + (\hat{y}_\beta - \hat{y}_\alpha)(y_\beta - y_\alpha) + (\hat{z}_\beta - \hat{z}_\alpha)(z_\beta - z_\alpha)](\hat{y}_\beta - \hat{y}_\alpha)}{(\hat{x}_\beta - \hat{x}_\alpha)^2 + (\hat{y}_\beta - \hat{y}_\alpha)^2 + (\hat{z}_\beta - \hat{z}_\alpha)^2} =$$

$$\sum_{\beta} \frac{k_{\alpha\beta} r^0_{\alpha\beta} (\hat{y}_\beta - \hat{y}_\alpha)}{\sqrt{(\hat{x}_\beta - \hat{x}_\alpha)^2 + (\hat{y}_\beta - \hat{y}_\alpha)^2 + (\hat{z}_\beta - \hat{z}_\alpha)^2}}$$

and in z direction

$$\sum_{\beta} \frac{k_{\alpha\beta}[(\hat{x}_\beta - \hat{x}_\alpha)(x_\beta - x_\alpha) + (\hat{y}_\beta - \hat{y}_\alpha)(y_\beta - y_\alpha) + (\hat{z}_\beta - \hat{z}_\alpha)(z_\beta - z_\alpha)](\hat{z}_\beta - \hat{z}_\alpha)}{(\hat{x}_\beta - \hat{x}_\alpha)^2 + (\hat{y}_\beta - \hat{y}_\alpha)^2 + (\hat{z}_\beta - \hat{z}_\alpha)^2} =$$

$$\sum_{\beta} \frac{k_{\alpha\beta} r^0_{\alpha\beta} (\hat{z}_\beta - \hat{z}_\alpha)}{\sqrt{(\hat{x}_\beta - \hat{x}_\alpha)^2 + (\hat{y}_\beta - \hat{y}_\alpha)^2 + (\hat{z}_\beta - \hat{z}_\alpha)^2}} = 0$$

3.1.2 Nonlinear models

There are two non-linear models under consideration.

(1) In the first non-linear model, the intermolecular forces $\mathbf{F}_{\alpha\beta}$ are still linear but large deformations are assumed. It implies that directions of the spring forces are now aligned with $\mathbf{x}_\beta - \mathbf{x}_\alpha$. Thus, the non-linearity of the model is a consequence of large deformations.

(2) In the second non-linear model we allow for large deformations and all the force potential functions $V(r_{\alpha\beta})$ are assumed to be non-linear, of the Lennard-Jones type [4]

$$V(r_{\alpha\beta}) = C_{\alpha\beta}[\left(\frac{\sigma_{\alpha\beta}}{r_{\alpha\beta}}\right)^{n_{\alpha\beta}} - \left(\frac{\sigma_{\alpha\beta}}{r_{\alpha\beta}}\right)^{m_{\alpha\beta}}] \tag{3}$$

Thus, for each spring we need data on the four parameters $C_{\alpha\beta}$, $\sigma_{\alpha\beta}$, $m_{\alpha\beta}$ and $n_{\alpha\beta}$.

Equilibrium equations for the non-linear model with quadratic potentials

At each particle α, force equilibrium has to hold. Thus

$$\sum_{\beta} \mathbf{F}^{\alpha}_{\alpha\beta} = 0, \quad \alpha = 1, 2, ..., N$$

which can be rewritten as

$$\mathbf{F}(\mathbf{X}) = 0$$

where $\mathbf{F}$ is a composition of $\mathbf{F}^\alpha$ for all $\alpha = 1, 2, ..., N$, and $\mathbf{X}$ is a composition of $x_1, x_2, ..., x_N$.

Using a Taylor expansion of $\mathbf{F}$ around a guess vector $\mathbf{X}^i$ we have

$$\mathbf{F}(\mathbf{X}) = \mathbf{F}(\mathbf{X}^i) + \partial\mathbf{F}(\mathbf{X}^i, \Delta\mathbf{X}^i) + H.O.T. \tag{4}$$

where $\mathbf{X} = \mathbf{X}^i + \Delta\mathbf{X}^i$ and $H.O.T.$ is an abreviation for higher order terms. Since

$$\mathbf{F}(\mathbf{X}) \approx \mathbf{F}(\mathbf{X}^i) + \partial\mathbf{F}(\mathbf{X}^i, \Delta\mathbf{X}^i). \tag{5}$$

then $\Delta\mathbf{X}^i$ can be approximated from

$$\partial\mathbf{F}(\mathbf{X}^i, \Delta\mathbf{X}^i) = -\mathbf{F}(\mathbf{X}^i). \tag{6}$$

and

$$\mathbf{F}(\mathbf{X}^i) = \sum_\beta \mathbf{F}_{\alpha\beta}(\mathbf{x}^i_\alpha, \mathbf{x}^i_\beta) = \sum_\beta k_{\alpha\beta}(\|\mathbf{x}^i_\beta - \mathbf{x}^i_\alpha\| - r^0_{\alpha\beta}) \cdot \frac{\mathbf{x}^i_\beta - \mathbf{x}^i_\alpha}{\|\mathbf{x}^i_\beta - \mathbf{x}^i_\alpha\|}$$

Here $\mathbf{x}^i_\alpha = (x^i_\alpha, y^i_\alpha, z^i_\alpha)$ and $\|\mathbf{x}^i_\alpha\| = \sqrt{(x^i_\alpha)^2 + (y^i_\alpha)^2 + (z^i_\alpha)^2}$.

We now derive the formula for the Jacobian

$$\partial\mathbf{F}(\mathbf{X}^i, \Delta\mathbf{X}^i) = \sum_\beta \partial\mathbf{F}_{\alpha\beta}(\mathbf{x}^i_\alpha, \mathbf{x}^i_\beta; \Delta\mathbf{x}^i_\alpha, \Delta\mathbf{x}^i_\beta)$$

By definition $\partial\mathbf{F}_{\alpha\beta}(\mathbf{x}^i_\alpha, \mathbf{x}^i_\beta; \Delta\mathbf{x}^i_\alpha, \Delta\mathbf{x}^i_\beta)$ is given by

$$\begin{aligned}
&\lim_{\theta\to 0}\frac{1}{\theta}[\mathbf{F}_{\alpha\beta}(\mathbf{x}^i_\alpha + \theta\Delta\mathbf{x}^i_\alpha, \mathbf{x}^i_\beta + \theta\Delta\mathbf{x}^i_\beta) - \mathbf{F}_{\alpha\beta}(\mathbf{x}^i_\alpha, \mathbf{x}^i_\beta)] \\
&= \lim_{\theta\to 0}\frac{1}{\theta}[k_{\alpha\beta}(\|\mathbf{x}^i_\beta + \theta\Delta\mathbf{x}^i_\beta - \mathbf{x}^i_\alpha - \theta\Delta\mathbf{x}^i_\alpha\| - r^0_{\alpha\beta})\frac{\mathbf{x}^i_\beta + \theta\Delta\mathbf{x}^i_\beta - \mathbf{x}^i_\alpha - \theta\Delta\mathbf{x}^i_\alpha}{\|\mathbf{x}^i_\beta + \theta\Delta\mathbf{x}^i_\beta - \mathbf{x}^i_\alpha - \theta\Delta\mathbf{x}^i_\alpha\|} \\
&\qquad - k_{\alpha\beta}(\|\mathbf{x}^i_\beta - \mathbf{x}^i_\alpha\| - r^0_{\alpha\beta})\frac{\mathbf{x}^i_\beta - \mathbf{x}^i_\alpha}{\|\mathbf{x}^i_\beta - \mathbf{x}^i_\alpha\|}] \\
&= \lim_{\theta\to 0}[k_{\alpha\beta}(\|\mathbf{x}^i_\beta - \mathbf{x}^i_\alpha + \theta(\Delta\mathbf{x}^i_\beta - \Delta\mathbf{x}^i_\alpha)\| - r^0_{\alpha\beta})]\frac{\Delta\mathbf{x}^i_\beta - \Delta\mathbf{x}^i_\alpha}{\|\mathbf{x}^i_\beta - \mathbf{x}^i_\alpha + \theta(\Delta\mathbf{x}^i_\beta - \Delta\mathbf{x}^i_\alpha)\|} \\
&\qquad + \lim_{\theta\to 0}\frac{1}{\theta}[k_{\alpha\beta}\|\mathbf{x}^i_\beta - \mathbf{x}^i_\alpha + \theta(\Delta\mathbf{x}^i_\beta - \Delta\mathbf{x}^i_\alpha)\|]\frac{\mathbf{x}^i_\beta - \mathbf{x}^i_\alpha}{\|\mathbf{x}^i_\beta - \mathbf{x}^i_\alpha + \theta(\Delta\mathbf{x}^i_\beta - \Delta\mathbf{x}^i_\alpha)\|} \\
&\qquad - \lim_{\theta\to 0}\frac{1}{\theta}k_{\alpha\beta}[\|\mathbf{x}^i_\beta - \mathbf{x}^i_\alpha\|]\frac{\mathbf{x}^i_\beta - \mathbf{x}^i_\alpha}{\|\mathbf{x}^i_\beta - \mathbf{x}^i_\alpha\|} \\
&\qquad - \lim_{\theta\to 0}\frac{1}{\theta}k_{\alpha\beta}r^0_{\alpha\beta}[\frac{1}{\|\mathbf{x}^i_\beta - \mathbf{x}^i_\alpha + \theta(\Delta\mathbf{x}^i_\beta - \Delta\mathbf{x}^i_\alpha)\|} - \frac{1}{\|\mathbf{x}^i_\beta - \mathbf{x}^i_\alpha\|}](\mathbf{x}^i_\beta - \mathbf{x}^i_\alpha) \\
&\qquad = k_{\alpha\beta}[\|\mathbf{x}^i_\beta - \mathbf{x}^i_\alpha\| - r^0_{\alpha\beta}]\frac{\Delta\mathbf{x}^i_\beta - \Delta\mathbf{x}^i_\alpha}{\|\mathbf{x}^i_\beta - \mathbf{x}^i_\alpha\|} \\
&\qquad - \lim_{\theta\to 0}\frac{1}{\theta}k_{\alpha\beta}r^0_{\alpha\beta}[\frac{\|\mathbf{x}^i_\beta - \mathbf{x}^i_\alpha\|^2 - \|\mathbf{x}^i_\beta - \mathbf{x}^i_\alpha + \theta(\Delta\mathbf{x}^i_\beta - \Delta\mathbf{x}^i_\alpha)\|^2}{\|\mathbf{x}^i_\beta - \mathbf{x}^i_\alpha\| + \|\mathbf{x}^i_\beta - \mathbf{x}^i_\alpha + \theta(\Delta\mathbf{x}^i_\beta - \Delta\mathbf{x}^i_\alpha)\|}] \\
&\qquad \cdot\frac{\mathbf{x}^i_\beta - \mathbf{x}^i_\alpha}{\|\mathbf{x}^i_\beta - \mathbf{x}^i_\alpha\| \cdot \|\mathbf{x}^i_\beta - \mathbf{x}^i_\alpha + \theta(\Delta\mathbf{x}^i_\beta - \Delta\mathbf{x}^i_\alpha)\|}
\end{aligned} \tag{7}$$

$$
\begin{aligned}
&= k_{\alpha\beta}[\|\mathbf{x}^i_\beta - \mathbf{x}^i_\alpha\| - r^0_{\alpha\beta}]\frac{\Delta\mathbf{x}^i_\beta - \Delta\mathbf{x}^i_\alpha}{\|\mathbf{x}^i_\beta - \mathbf{x}^i_\alpha\|} \\
&- \lim_{\theta\to 0}\frac{1}{\theta}k_{\alpha\beta}r^0_{\alpha\beta}[\frac{-2\theta(\mathbf{x}^i_\beta - \mathbf{x}^i_\alpha)\cdot(\Delta\mathbf{x}^i_\beta - \Delta\mathbf{x}^i_\alpha) - \theta^2\|\Delta\mathbf{x}^i_\beta - \Delta\mathbf{x}^i_\alpha\|^2}{\|\mathbf{x}^i_\beta - \mathbf{x}^i_\alpha\| + \|\mathbf{x}^i_\beta - \mathbf{x}^i_\alpha + \theta(\Delta\mathbf{x}^i_\beta - \Delta\mathbf{x}^i_\alpha)\|}] \\
&\cdot\frac{\mathbf{x}^i_\beta - \mathbf{x}^i_\alpha}{\|\mathbf{x}^i_\beta - \mathbf{x}^i_\alpha\|\cdot\|\mathbf{x}^i_\beta - \mathbf{x}^i_\alpha + \theta(\Delta\mathbf{x}^i_\beta - \Delta\mathbf{x}^i_\alpha)\|} \\
= k_{\alpha\beta}[\|\mathbf{x}^i_\beta - \mathbf{x}^i_\alpha\| - r^0_{\alpha\beta}]&\frac{\Delta\mathbf{x}^i_\beta - \Delta\mathbf{x}^i_\alpha}{\|\mathbf{x}^i_\beta - \mathbf{x}^i_\alpha\|} + k_{\alpha\beta}r^0_{\alpha\beta}[\frac{(\mathbf{x}^i_\beta - \mathbf{x}^i_\alpha)\cdot(\Delta\mathbf{x}^i_\beta - \Delta\mathbf{x}^i_\alpha)}{\|\mathbf{x}^i_\beta - \mathbf{x}^i_\alpha\|^2}]\cdot\frac{\mathbf{x}^i_\beta - \mathbf{x}^i_\alpha}{\|\mathbf{x}^i_\beta - \mathbf{x}^i_\alpha\|}
\end{aligned}
\tag{8}
$$

We can reformulate the equations in matrix-vector notation, i.e.

$$
\partial\mathbf{F}_{\alpha\beta}(\mathbf{X}^i;\Delta\mathbf{X}^i) = \begin{pmatrix}\mathbf{K}^{\alpha\alpha} & \mathbf{K}^{\alpha\beta}\end{pmatrix}\begin{pmatrix}\Delta\mathbf{x}^i_\alpha \\ \Delta\mathbf{x}^i_\beta\end{pmatrix} \tag{9}
$$

In the following, we use Einstein's notation $a_ib_i = a_1b_1 + a_2b_2 + a_3b_3$. We define the Cartesian base vectors $\mathbf{e}_1 = (1,0,0)$, $\mathbf{e}_2 = (0,1,0)$, and $\mathbf{e}_3 = (0,0,1)$. Hence $\mathbf{b} = b_i\mathbf{e}_i$ and $\mathbf{a}\cdot\mathbf{b} = (a_i\mathbf{e}_i)\cdot(b_j\mathbf{e}_j) = a_ib_j(\mathbf{e}_i\cdot\mathbf{e}_j) = a_ib_j\delta_{ij} = a_{ii}$. Now we can write

$$
\begin{array}{ll}
\Delta\mathbf{x}^i_\alpha = \Delta\xi^i_{\alpha,j}\mathbf{e}_j & \mathbf{x}^i_\alpha = \xi^i_{\alpha,j}\mathbf{e}_j \\
\underbrace{\Delta\mathbf{x}^i_\beta = \Delta\xi^i_{\beta,j}\mathbf{e}_j} & \underbrace{\mathbf{x}^i_\beta = \xi^i_{\beta,j}\mathbf{e}_j} \\
\text{unknown} & \text{known}
\end{array}
$$

Furthermore, for simplicity in the notation, we define

$$
\Phi^i_{\alpha\beta} = k_{\alpha\beta}\frac{[\|\mathbf{x}^i_\beta - \mathbf{x}^i_\alpha\| - r^0_{\alpha\beta}]}{\|\mathbf{x}^i_\beta - \mathbf{x}^i_\alpha\|}
$$

and

$$
\varphi^i_{\alpha\beta} = \frac{k_{\alpha\beta}r^0_{\alpha\beta}}{\|\mathbf{x}^i_\beta - \mathbf{x}^i_\alpha\|^3}
$$

Now, we can rewrite equation (8)

$$\begin{aligned}\partial \mathbf{F}_{\alpha\beta} &= \Phi^i_{\alpha\beta}(\Delta\xi^i_{\beta,j} - \Delta\xi^i_{\alpha,j})\mathbf{e}_j + \varphi^i_{\alpha\beta}[(\xi^i_{\beta,k} - \xi^i_{\alpha,k})\mathbf{e}_k \cdot (\xi^i_{\beta,l} - \xi^i_{\alpha,l})\mathbf{e}_l](\xi^i_{\beta,j} - \xi^i_{\alpha,j})\mathbf{e}_j \\ &= \left(\Phi^i_{\alpha\beta}(\Delta\xi^i_{\beta,j} - \Delta\xi^i_{\alpha,j}) + \varphi^i_{\alpha\beta}[\xi^i_{\beta,l}\Delta\xi^i_{\beta,l} - \xi^i_{\beta,l}\Delta\xi^i_{\alpha,l} - \xi^i_{\alpha,l}\Delta\xi^i_{\beta,l} + \Delta\xi^i_{\alpha,l}\xi^i_{\alpha,l}] \times (\xi^i_{\beta,j} - \xi^i_{\alpha,j})\right)\mathbf{e}_j \\ &= \left(-[\Phi^i_{\alpha\beta} + \varphi^i_{\alpha\beta}(\xi^i_{\beta,j} - \Delta\xi^i_{\alpha,j})^2]\Delta\xi^i_{\alpha,j} - \sum_{l\neq j}\varphi^i_{\alpha\beta}(\xi^i_{\beta,l} - \xi^i_{\alpha,l})(\xi^i_{\beta,j} - \xi^i_{\alpha,j})\Delta\xi^i_{\alpha,l}\right. \\ &\quad \left. + [\Phi^i_{\alpha\beta} + \varphi^i_{\alpha\beta}(\xi^i_{\beta,j} - \xi^i_{\alpha,j})^2]\Delta\xi^i_{\beta,j} + \sum_{l\neq j}\varphi^i_{\alpha\beta}(\xi^i_{\beta,l} - \xi^i_{\alpha,l})(\xi^i_{\beta,j} - \xi^i_{\alpha,j})\Delta\xi^i_{\beta,l}\right)\mathbf{e}_j\end{aligned} \tag{10}$$

Thus

$$\mathbf{K}^{\alpha\alpha} = \begin{pmatrix} -(\Phi^i_{\alpha\beta} + \varphi^i_{\alpha\beta}(x^i_\beta - x^i_\alpha)^2) & -\varphi^i_{\alpha\beta}(y^i_\beta - y^i_\alpha)(x^i_\beta - x^i_\alpha) & -\varphi^i_{\alpha\beta}(z^i_\beta - z^i_\alpha)(x^i_\beta - x^i_\alpha) \\ -\varphi^i_{\alpha\beta}(x^i_\beta - x^i_\alpha)(y^i_\beta - y^i_\alpha) & -(\Phi^i_{\alpha\beta} + \varphi^i_{\alpha\beta}(y^i_\beta - y^i_\alpha)^2) & -\varphi^i_{\alpha\beta}(y^i_\beta - y^i_\alpha)(z^i_\beta - z^i_\alpha) \\ -\varphi^i_{\alpha\beta}(x^i_\beta - x^i_\alpha)(z^i_\beta - z^i_\alpha) & -\varphi^i_{\alpha\beta}(y^i_\beta - y^i_\alpha)(z^i_\beta - z^i_\alpha) & -(\Phi^i_{\alpha\beta} + \varphi^i_{\alpha\beta}(z^i_\beta - z^i_\alpha)^2) \end{pmatrix}$$

where submatrices are located in α and β rows and columns.

$$\mathbf{K} = \begin{pmatrix} \mathbf{K}^{\alpha\alpha} & \mathbf{K}^{\alpha\beta} \\ \mathbf{K}^{\beta\alpha} & \mathbf{K}^{\beta\beta} \end{pmatrix}$$

and $\mathbf{K}^{\alpha\beta} = -\mathbf{K}^{\alpha\alpha}$, $\mathbf{K}^{\beta\beta} = \mathbf{K}^{\alpha\alpha}$, $\mathbf{K}^{\beta\alpha} = \mathbf{K}^{\alpha\beta}$.

Equilibrium equations for the non-linear model with Lennard-Jones potentials

At each particle α, force equilibrium has to hold. Thus

$$\mathbf{R}_\alpha = \sum_\beta \mathbf{F}^\alpha_{\alpha\beta} = 0, \quad \alpha = 1, 2, ..., N$$

Collection of all resultant forces is

$$\mathbf{F} = \begin{pmatrix} \mathbf{R_1} \\ \mathbf{R_2} \\ ... \\ \mathbf{R_N} \end{pmatrix} = \mathbf{0}$$

where $\mathbf{F} = \mathbf{F}(\mathbf{X})$ and $\mathbf{X}$ is a vector in $\mathbf{R}^N$ with components $x_1, x_2, ..., x_N$.

The force exerted by all neighboring particles β on a particle α is given by

$$\mathbf{F}(\mathbf{X}^i) = \sum_\beta \mathbf{F}_{\alpha\beta}(\mathbf{x}^i_\alpha, \mathbf{x}^i_\beta) = \sum_\beta |\mathbf{F}_{\alpha\beta}| \frac{\mathbf{x}^i_\beta - \mathbf{x}^i_\alpha}{\|\mathbf{x}^i_\beta - \mathbf{x}^i_\alpha\|}$$

where

$$|\mathbf{F}_{\alpha\beta}| = -\frac{\partial V}{\partial r}$$

and $V(r)$ is the Lennard-Jones potential function given by (3).

Since

$$\frac{\partial V(r)}{\partial r} = C_{\alpha\beta}[\frac{m_{\alpha\beta}}{\sigma_{\alpha\beta}} \left(\frac{\sigma_{\alpha\beta}}{r}\right)^{m_{\alpha\beta}-1} - \frac{n_{\alpha\beta}}{\sigma_{\alpha\beta}} \left(\frac{\sigma_{\alpha\beta}}{r}\right)^{n_{\alpha\beta}-1}]$$

thus

$$\mathbf{R}_\alpha(\mathbf{X}^i) = -\sum_\beta \frac{C_{\alpha\beta}}{\sigma_{\alpha\beta}} [m_{\alpha\beta} \left(\frac{\sigma_{\alpha\beta}}{\|\mathbf{x}^i_\beta - \mathbf{x}^i_\alpha\|}^{m_{\alpha\beta}+1}\right) - n_{\alpha\beta} \left(\frac{\sigma_{\alpha\beta}}{\|\mathbf{x}^i_\beta - \mathbf{x}^i_\alpha\|}^{n_{\alpha\beta}+1}\right)] \times \frac{\mathbf{x}^i_\beta - \mathbf{x}^i_\alpha}{\|\mathbf{x}^i_\beta - \mathbf{x}^i_\alpha\|}$$

We will compute the Jacobian $\partial\mathbf{F}$. Since

$$\partial\mathbf{F} = \begin{pmatrix} \partial\mathbf{R_1} \\ ... \\ \partial\mathbf{R_N} \end{pmatrix}$$

and

$$\partial\mathbf{R}_\alpha = \sum_\beta \partial\mathbf{F}_{\alpha\beta}$$

then we need to compute

$$\partial\mathbf{F}_{\alpha\beta}(\partial\mathbf{X}^i, \Delta\partial\mathbf{X}^i) = \lim_{\theta\to 0} \frac{1}{\theta} \left(\mathbf{F}_{\alpha\beta}(\partial\mathbf{X}^i + \theta\Delta\partial\mathbf{X}^i) - \mathbf{F}_{\alpha\beta}(\partial\mathbf{X}^i)\right)$$

We will focus on $\mathbf{F}_{\alpha\beta}(\partial\mathbf{X}^i + \theta\Delta\partial\mathbf{X}^i)$ first.

$$\lim_{\theta\to 0}\frac{1}{\theta}\mathbf{F}_{\alpha\beta}(\partial\mathbf{X}^i+\theta\Delta\partial\mathbf{X}^i)$$
$$=-\lim_{\theta\to 0}\frac{1}{\theta}\left(\frac{C_{\alpha\beta}}{\sigma_{\alpha\beta}}[m_{\alpha\beta}(\frac{\sigma_{\alpha\beta}}{\|\mathbf{x}^i_\beta-\mathbf{x}^i_\alpha+\theta(\Delta\mathbf{x}^i_\beta-\Delta\mathbf{x}^i_\alpha)\|})^{m_{\alpha\beta}+1}\right.$$
$$\left.-n_{\alpha\beta}(\frac{\sigma_{\alpha\beta}}{\|\mathbf{x}^i_\beta-\mathbf{x}^i_\alpha+\theta(\Delta\mathbf{x}^i_\beta-\Delta\mathbf{x}^i_\alpha)\|})^{n_{\alpha\beta}+1}]\ \frac{\mathbf{x}^i_\beta-\mathbf{x}^i_\alpha+\theta(\Delta\mathbf{x}^i_\beta-\Delta\mathbf{x}^i_\alpha)}{\|\mathbf{x}^i_\beta-\mathbf{x}^i_\alpha+\theta(\Delta\mathbf{x}^i_\beta-\Delta\mathbf{x}^i_\alpha)\|}\right)$$
$$=-\lim_{\theta\to 0}\frac{1}{\theta}\left(\frac{C_{\alpha\beta}}{\sigma_{\alpha\beta}}[m_{\alpha\beta}(\frac{\sigma_{\alpha\beta}}{\|\mathbf{x}^i_\beta-\mathbf{x}^i_\alpha+\theta(\Delta\mathbf{x}^i_\beta-\Delta\mathbf{x}^i_\alpha)\|})^{m_{\alpha\beta}+1}\right.$$
$$-n_{\alpha\beta}(\frac{\sigma_{\alpha\beta}}{\|\mathbf{x}^i_\beta-\mathbf{x}^i_\alpha+\theta(\Delta\mathbf{x}^i_\beta-\Delta\mathbf{x}^i_\alpha)\|})^{n_{\alpha\beta}+1}]\ \frac{\mathbf{x}^i_\beta-\mathbf{x}^i_\alpha}{\|\mathbf{x}^i_\beta-\mathbf{x}^i_\alpha+\theta(\Delta\mathbf{x}^i_\beta-\Delta\mathbf{x}^i_\alpha)\|}$$
$$-C_{\alpha\beta}\sigma_{\alpha\beta}[m_{\alpha\beta}(\frac{\sigma_{\alpha\beta}}{\|\mathbf{x}^i_\beta-\mathbf{x}^i_\alpha+\theta(\Delta\mathbf{x}^i_\beta-\Delta\mathbf{x}^i_\alpha)\|})^{m_{\alpha\beta}+1}$$
$$\left.-n_{\alpha\beta}(\frac{\sigma_{\alpha\beta}}{\|\mathbf{x}^i_\beta-\mathbf{x}^i_\alpha+\theta(\Delta\mathbf{x}^i_\beta-\Delta\mathbf{x}^i_\alpha)\|})^{n_{\alpha\beta}+1}]\ \frac{\Delta\mathbf{x}^i_\beta-\Delta\mathbf{x}^i_\alpha}{\|\mathbf{x}^i_\beta-\mathbf{x}^i_\alpha+\theta(\Delta\mathbf{x}^i_\beta-\Delta\mathbf{x}^i_\alpha)\|}\right) \tag{11}$$

$$=\lim_{\theta\to 0}\frac{C_{\alpha\beta}m_{\alpha\beta}\sigma_{\alpha\beta}^{m_{\alpha\beta}}}{\theta}\left(\frac{\|\mathbf{x}^i_\beta-\mathbf{x}^i_\alpha\|}{\|\mathbf{x}^i_\beta-\mathbf{x}^i_\alpha+\theta(\Delta\mathbf{x}^i_\beta-\Delta\mathbf{x}^i_\alpha)\|^{m_{\alpha\beta}+1}}\right.$$
$$\left.-\frac{\|\mathbf{x}^i_\beta-\mathbf{x}^i_\alpha+\theta(\Delta\mathbf{x}^i_\beta-\Delta\mathbf{x}^i_\alpha)\|}{\|\mathbf{x}^i_\beta-\mathbf{x}^i_\alpha\|^{m_{\alpha\beta}+1}}\right)\frac{\mathbf{x}^i_\beta-\mathbf{x}^i_\alpha}{\|\mathbf{x}^i_\beta-\mathbf{x}^i_\alpha\|\|\mathbf{x}^i_\beta-\mathbf{x}^i_\alpha+\theta(\Delta\mathbf{x}^i_\beta-\Delta\mathbf{x}^i_\alpha)\|} \tag{12}$$

$$+\lim_{\theta\to 0}\frac{C_{\alpha\beta}n_{\alpha\beta}\sigma_{\alpha\beta}^{n_{\alpha\beta}}}{\theta}\left(\frac{\|\mathbf{x}^i_\beta-\mathbf{x}^i_\alpha\|}{\|\mathbf{x}^i_\beta-\mathbf{x}^i_\alpha+\theta(\Delta\mathbf{x}^i_\beta-\Delta\mathbf{x}^i_\alpha)\|^{n_{\alpha\beta}+1}}\right.$$
$$\left.-\frac{\|\mathbf{x}^i_\beta-\mathbf{x}^i_\alpha+\theta(\Delta\mathbf{x}^i_\beta-\Delta\mathbf{x}^i_\alpha)\|}{\|\mathbf{x}^i_\beta-\mathbf{x}^i_\alpha\|^{n_{\alpha\beta}+1}}\right)\frac{\mathbf{x}^i_\beta-\mathbf{x}^i_\alpha}{\|\mathbf{x}^i_\beta-\mathbf{x}^i_\alpha\|\|\mathbf{x}^i_\beta-\mathbf{x}^i_\alpha+\theta(\Delta\mathbf{x}^i_\beta-\Delta\mathbf{x}^i_\alpha)\|} \tag{13}$$

Let us focus on term (12) now

$$\lim_{\theta\to 0}\frac{C_{\alpha\beta}m_{\alpha\beta}\sigma_{\alpha\beta}^{m_{\alpha\beta}}}{\theta}\left(\|\mathbf{x}^i_\beta-\mathbf{x}^i_\alpha\|^{m_{\alpha\beta}+2}-\|\mathbf{x}^i_\beta-\mathbf{x}^i_\alpha+\theta(\Delta\mathbf{x}^i_\beta-\Delta\mathbf{x}^i_\alpha)\|^{m_{\alpha\beta}+2}\right)$$
$$\times\frac{\mathbf{x}^i_\beta-\mathbf{x}^i_\alpha}{\|\mathbf{x}^i_\beta-\mathbf{x}^i_\alpha\|^{m_{\alpha\beta}+2}\|\mathbf{x}^i_\beta-\mathbf{x}^i_\alpha+\theta(\Delta\mathbf{x}^i_\beta-\Delta\mathbf{x}^i_\alpha)\|^{m_{\alpha\beta}+2}} \tag{14}$$

$$= \lim_{\theta \to 0} \frac{C_{\alpha\beta} m_{\alpha\beta} \sigma_{\alpha\beta}^{m_{\alpha\beta}}}{\theta} \left(\|\mathbf{x}_\beta^i - \mathbf{x}_\alpha^i\|^{2(m_{\alpha\beta}+2)} - \|\mathbf{x}_\beta^i - \mathbf{x}_\alpha^i + \theta(\Delta\mathbf{x}_\beta^i - \Delta\mathbf{x}_\alpha^i)\|^{2(m_{\alpha\beta}+2)} \right) \times \frac{\mathbf{x}_\beta^i - \mathbf{x}_\alpha^i}{\|\mathbf{x}_\beta^i - \mathbf{x}_\alpha^i\|^{m_{\alpha\beta}+2} \|\mathbf{x}_\beta^i - \mathbf{x}_\alpha^i + \theta(\Delta\mathbf{x}_\beta^i - \Delta\mathbf{x}_\alpha^i)\|^{m_{\alpha\beta}+2}} \times \frac{1}{[\|\mathbf{x}_\beta^i - \mathbf{x}_\alpha^i\|^{m_{\alpha\beta}+2} + \|\mathbf{x}_\beta^i - \mathbf{x}_\alpha^i + \theta(\Delta\mathbf{x}_\beta^i - \Delta\mathbf{x}_\alpha^i)\|^{m_{\alpha\beta}+2}]} \tag{15}$$

$$= \lim_{\theta \to 0} \frac{C_{\alpha\beta} m_{\alpha\beta} \sigma_{\alpha\beta}^{m_{\alpha\beta}}}{\theta} \left(\|\mathbf{x}_\beta^i - \mathbf{x}_\alpha^i\|^{2(m_{\alpha\beta}+2)} - (\|\mathbf{x}_\beta^i - \mathbf{x}_\alpha^i\|^2 + 2\theta(\Delta\mathbf{x}_\beta^i - \Delta\mathbf{x}_\alpha^i) \cdot (\mathbf{x}_\beta^i - \mathbf{x}_\alpha^i) + \theta^2 \|\Delta\mathbf{x}_\beta^i - \Delta\mathbf{x}_\alpha^i\|^2)^{m_{\alpha\beta}+2} \right) \times \frac{\mathbf{x}_\beta^i - \mathbf{x}_\alpha^i}{\|\mathbf{x}_\beta^i - \mathbf{x}_\alpha^i\|^{m_{\alpha\beta}+2} \|\mathbf{x}_\beta^i - \mathbf{x}_\alpha^i + \theta(\Delta\mathbf{x}_\beta^i - \Delta\mathbf{x}_\alpha^i)\|^{m_{\alpha\beta}+2}} \times \frac{1}{[\|\mathbf{x}_\beta^i - \mathbf{x}_\alpha^i\|^{m_{\alpha\beta}+2} + \|\mathbf{x}_\beta^i - \mathbf{x}_\alpha^i + \theta(\Delta\mathbf{x}_\beta^i - \Delta\mathbf{x}_\alpha^i)\|^{m_{\alpha\beta}+2}]} \tag{16}$$

We can cancel out terms, and take the limit

$$= \lim_{\theta \to 0} \frac{C_{\alpha\beta} m_{\alpha\beta} \sigma_{\alpha\beta}^{m_{\alpha\beta}}}{\theta} \left(\|\mathbf{x}_\beta^i - \mathbf{x}_\alpha^i\|^{2(m_{\alpha\beta}+2)} - \|\mathbf{x}_\beta^i - \mathbf{x}_\alpha^i\|^{2(m_{\alpha\beta}+2)} - 2\theta(m_{\alpha\beta}+2)\|\mathbf{x}_\beta^i - \mathbf{x}_\alpha^i\|^{2m_{\alpha\beta}+3}(\mathbf{x}_\beta^i - \mathbf{x}_\alpha^i) \cdot (\Delta\mathbf{x}_\beta^i - \Delta\mathbf{x}_\alpha^i) + \bigcirc(\theta^2) \right) \times \frac{\mathbf{x}_\beta^i - \mathbf{x}_\alpha^i}{\|\mathbf{x}_\beta^i - \mathbf{x}_\alpha^i\|^{m_{\alpha\beta}+2} \|\mathbf{x}_\beta^i - \mathbf{x}_\alpha^i + \theta(\Delta\mathbf{x}_\beta^i - \Delta\mathbf{x}_\alpha^i)\|^{m_{\alpha\beta}+2}} \times \frac{1}{[\|\mathbf{x}_\beta^i - \mathbf{x}_\alpha^i\|^{m_{\alpha\beta}+2} + \|\mathbf{x}_\beta^i - \mathbf{x}_\alpha^i + \theta(\Delta\mathbf{x}_\beta^i - \Delta\mathbf{x}_\alpha^i)\|^{m_{\alpha\beta}+2}]} \tag{17}$$

$$= C_{\alpha\beta} m_{\alpha\beta} \sigma_{\alpha\beta}^{m_{\alpha\beta}} \left(2(m_{\alpha\beta}+2)\|\mathbf{x}_\beta^i - \mathbf{x}_\alpha^i\|^{2m_{\alpha\beta}+3}(\mathbf{x}_\beta^i - \mathbf{x}_\alpha^i) \cdot (\Delta\mathbf{x}_\beta^i - \Delta\mathbf{x}_\alpha^i) \right) \times \frac{\mathbf{x}_\beta^i - \mathbf{x}_\alpha^i}{2\|\mathbf{x}_\beta^i - \mathbf{x}_\alpha^i\|^{3(m_{\alpha\beta}+2)}} \tag{18}$$

$$= C_{\alpha\beta} m_{\alpha\beta} (m_{\alpha\beta}+2) \sigma_{\alpha\beta}^{m_{\alpha\beta}} \frac{(\mathbf{x}_\beta^i - \mathbf{x}_\alpha^i) \cdot (\Delta\mathbf{x}_\beta^i - \Delta\mathbf{x}_\alpha^i)}{\|\mathbf{x}_\beta^i - \mathbf{x}_\alpha^i\|^{m_{\alpha\beta}+3}} (\mathbf{x}_\beta^i - \mathbf{x}_\alpha^i)$$

$$= \frac{C_{\alpha\beta} m_{\alpha\beta} (m_{\alpha\beta}+2)}{\sigma_{\alpha\beta}^3} \left(\frac{\sigma_{\alpha\beta}}{\|\mathbf{x}_\beta^i - \mathbf{x}_\alpha^i\|} \right)^{m_{\alpha\beta}+3} (\mathbf{x}_\beta^i - \mathbf{x}_\alpha^i) \cdot (\Delta\mathbf{x}_\beta^i - \Delta\mathbf{x}_\alpha^i)(\mathbf{x}_\beta^i - \mathbf{x}_\alpha^i) \tag{19}$$

Similarly, term (13)

$$= \frac{C_{\alpha\beta} n_{\alpha\beta} (n_{\alpha\beta}+2)}{\sigma_{\alpha\beta}^3} \left(\frac{\sigma_{\alpha\beta}}{\|\mathbf{x}_\beta^i - \mathbf{x}_\alpha^i\|} \right)^{n_{\alpha\beta}+3} (\mathbf{x}_\beta^i - \mathbf{x}_\alpha^i) \cdot (\Delta\mathbf{x}_\beta^i - \Delta\mathbf{x}_\alpha^i)(\mathbf{x}_\beta^i - \mathbf{x}_\alpha^i) \tag{20}$$

Let us focus on $\mathbf{F}_{\alpha\beta}(\partial\mathbf{X}^i)$ now

$$\lim_{\theta\to 0}\mathbf{F}_{\alpha\beta}(\partial\mathbf{X}^i)$$
$$= \lim_{\theta\to 0}\left(\frac{C_{\alpha\beta}}{\sigma_{\alpha\beta}}[m_{\alpha\beta}(\frac{\sigma_{\alpha\beta}}{\|\mathbf{x}^i_\beta-\mathbf{x}^i_\alpha\|}^{m_{\alpha\beta}+1}-n_{\alpha\beta}(\frac{\sigma_{\alpha\beta}}{\|\mathbf{x}^i_\beta-\mathbf{x}^i_\alpha\|}^{n_{\alpha\beta}+1})]\frac{\mathbf{x}^i_\beta-\mathbf{x}^i_\alpha}{\|\mathbf{x}^i_\beta-\mathbf{x}^i_\alpha\|}\right) \tag{21}$$

$$= -\frac{C_{\alpha\beta}}{\sigma_{\alpha\beta}}[m_{\alpha\beta}(\frac{\sigma_{\alpha\beta}}{\|\mathbf{x}^i_\beta-\mathbf{x}^i_\alpha\|})^{m_{\alpha\beta}+1}-n_{\alpha\beta}(\frac{\sigma_{\alpha\beta}}{\|\mathbf{x}^i_\beta-\mathbf{x}^i_\alpha\|})^{n_{\alpha\beta}+1}]\frac{\Delta\mathbf{x}^i_\beta-\Delta\mathbf{x}^i_\alpha}{\|\mathbf{x}^i_\beta-\mathbf{x}^i_\alpha\|} \tag{22}$$

We finally get

$$\partial\mathbf{F}_{\alpha\beta}(\partial\mathbf{X}^i,\Delta\partial\mathbf{X}^i)=\lim_{\theta\to 0}\frac{1}{\theta}\left(\mathbf{F}_{\alpha\beta}(\partial\mathbf{X}^i+\theta\Delta\partial\mathbf{X}^i)-\mathbf{F}_{\alpha\beta}(\partial\mathbf{X}^i)\right)$$
$$= \frac{C_{\alpha\beta}}{\sigma^3_{\alpha\beta}}\left(n_{\alpha\beta}(n_{\alpha\beta}+2)(\frac{\sigma_{\alpha\beta}}{\|\mathbf{x}^i_\beta-\mathbf{x}^i_\alpha\|})^{n_{\alpha\beta}+3}-m_{\alpha\beta}(m_{\alpha\beta}+2)(\frac{\sigma_{\alpha\beta}}{\|\mathbf{x}^i_\beta-\mathbf{x}^i_\alpha\|})^{m_{\alpha\beta}+3}\right)$$
$$\times(\mathbf{x}^i_\beta-\mathbf{x}^i_\alpha)\cdot(\Delta\mathbf{x}^i_\beta-\Delta\mathbf{x}^i_\alpha)(\mathbf{x}^i_\beta-\mathbf{x}^i_\alpha)$$
$$+\frac{C_{\alpha\beta}}{\sigma^2_{\alpha\beta}}[n_{\alpha\beta}(\frac{\sigma_{\alpha\beta}}{\|\mathbf{x}^i_\beta-\mathbf{x}^i_\alpha\|})^{n_{\alpha\beta}+2}-m_{\alpha\beta}(\frac{\sigma_{\alpha\beta}}{\|\mathbf{x}^i_\beta-\mathbf{x}^i_\alpha\|})^{m_{\alpha\beta}+2}]\times(\Delta\mathbf{x}^i_\beta-\Delta\mathbf{x}^i_\alpha) \tag{23}$$

Equation (23) can be written in matrix-vector form (9)

As in equation (8), we introduce the coefficients

$$\Phi^i_{\alpha\beta}=\frac{C_{\alpha\beta}}{\sigma_{\alpha\beta}}[n_{\alpha\beta}\left(\frac{\sigma_{\alpha\beta}}{\|\mathbf{x}^i_\beta-\mathbf{x}^i_\alpha\|}\right)^{n_{\alpha\beta}+2}-m_{\alpha\beta}\left(\frac{\sigma_{\alpha\beta}}{\|\mathbf{x}^i_\beta-\mathbf{x}^i_\alpha\|}\right)^{m_{\alpha\beta}+2}]$$

and

$$\varphi^i_{\alpha\beta}=\frac{C_{\alpha\beta}}{\sigma_{\alpha\beta}}[n_{\alpha\beta}(n_{\alpha\beta}+2)\left(\frac{\sigma_{\alpha\beta}}{\|\mathbf{x}^i_\beta-\mathbf{x}^i_\alpha\|}\right)^{n_{\alpha\beta}+3}-m_{\alpha\beta}(m_{\alpha\beta}+2)\left(\frac{\sigma_{\alpha\beta}}{\|\mathbf{x}^i_\beta-\mathbf{x}^i_\alpha\|}\right)^{m_{\alpha\beta}+3}]$$

Using this notation, equations (23) become

$$\partial\mathbf{F}_{\alpha\beta}(\mathbf{X}^i;\Delta\mathbf{X}^i)=\Phi_{\alpha\beta}(\Delta\mathbf{x}^i_\beta-\Delta\mathbf{x}^i_\alpha)+\varphi\left((\mathbf{x}^i_\beta-\mathbf{x}^i_\alpha)\cdot(\Delta\mathbf{x}^i_\beta-\Delta\mathbf{x}^i_\alpha)\right)\times(\mathbf{x}^i_\beta-\mathbf{x}^i_\alpha)$$

which is exactly the same equation we obtained using quadratic potential function.

3.2 Numerical analysis of the Molecular Statics Models

We consider a block of the feature containing $I_N \times J_N \times K_N$ cells. The particles are located at the grid nodes. Thus, the total number of particles is equal to $(I_N+1)\times(J_N+1)\times(K_N+1)$. We introduce integer (i,j,k) and real (x_i, y_j, z_k) coordinates for each particle $p_{i,j,k} = (x_i, y_j, z_k)$ (see Figure 3.2) Particles are

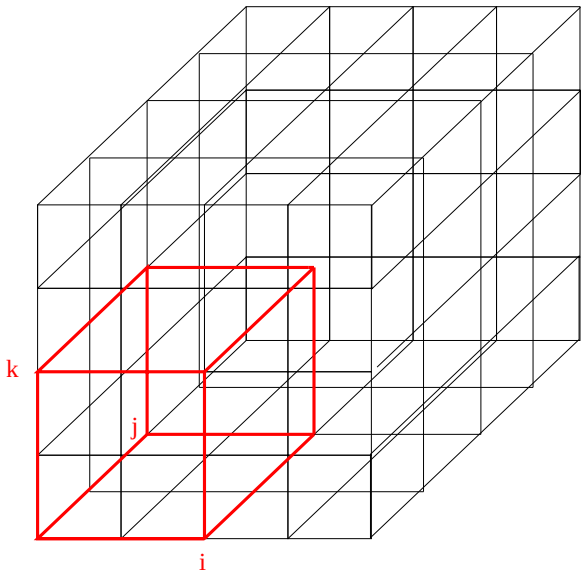

Fig. 3.2: Integer coordinates (i,j,k) of particle.

connected by bonds, which are modeled either by linear spring or non-linear Lennard-Jones force potential functions. The equilibrium equations are computed at each particle by considering the sum of the forces that are exerted by each neighboring particle, see Figure 3.2. Homogeneous displacements are applied for particles located in the base-plane of the feature.

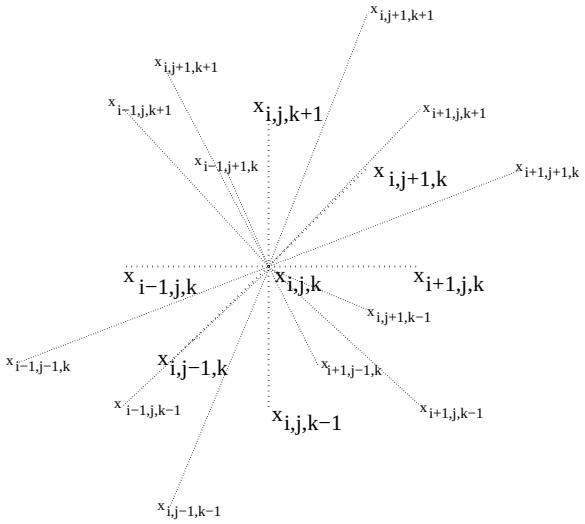

Fig. 3.3: Each particle interacts with its 27 neighbors.

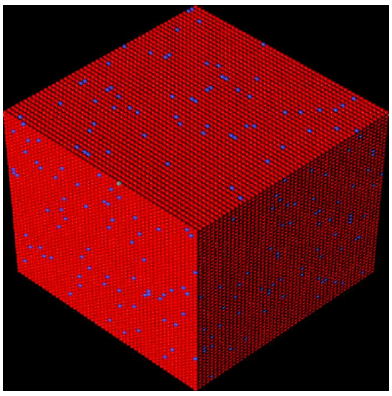

Fig. 3.4: Initial configuration of the grid.

Here, the numerical results are presented for three Molecular Statics Models in the case of two configurations of the feature: *before and after the template is released.*

Linear model with quadratic potentials, assuming small displacements

We have performed numerical simulation of the deformation of the feature inside the template. The grid of $50 \times 50 \times 50$ particles has been embedded inside additional layer of particles representing the template. Thus the total number of particles is $52 \times 52 \times 52$. The boundary conditions for the model are no displacement of particles located at base of the feature, and no displacement of template particles. The forces between the template particles and the feature particles describe interactions between the template and the feature.

The initial configuration of the grid is presented in Figure 3.4. The distribution of inter-particle potentials within the grid are obtained from a Monte-Carlo simulation of polymerization process [6].

We will consider here that the small displacement assumption is violated as soon as the displacements exceed ten percent of the distance between neighboring particles, in which case the results are deemed unphysical.

We have used the Preconditioned Conjugated Gradients (PCG) from the SLATEC library [7], with diagonal preconditioner. The total computations time is 87 second. The results are shown in Figure 3.5. We observe relatively small displacements of particles.

The next simulation is performed after removal of the template. We have removed additional layer of particles representing the template/feature interactions. Boundary condition are set to zero displacement at the base. No external forces or boundary conditions are prescribed on the other boundaries

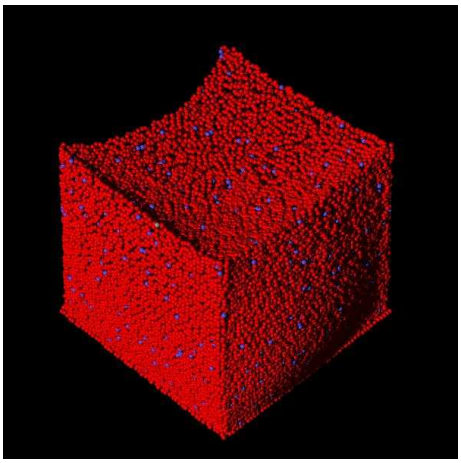

Fig. 3.5: Deformation of the feature inside the template provided by the linear model with quadratic potentials.

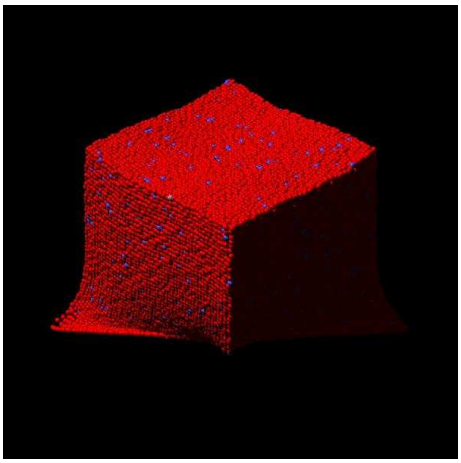

Fig. 3.6: Deformation of the feature outside the template provided by the linear model with quadratic potentials.

of the feature.

The total computational time is 207 second now. Large displacements for this case are observed and there is visible shrinkage of the feature. Moreover the feature has also twisted across the vertical axis of symmetry. This behaviour is unphysical, and we conclude that the linear model is anappropriate for such simulations.

Non-linear model with quadratic potentials, allowing for large displacements

In these experiments, the boundary conditions are the same as in the linear model discussed above. The difference now is that the non-linearity of the model requires the Newton-Raphson loop over the iterative solver. We used

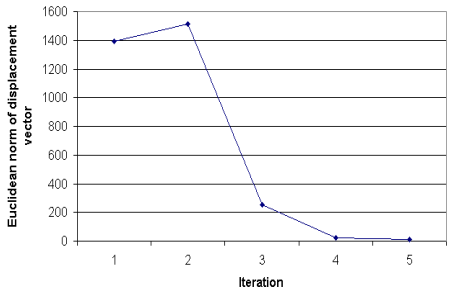

Fig. 3.7: Convergence history of GMRES solver solving non-linear case with quadratic potentials, inside template.

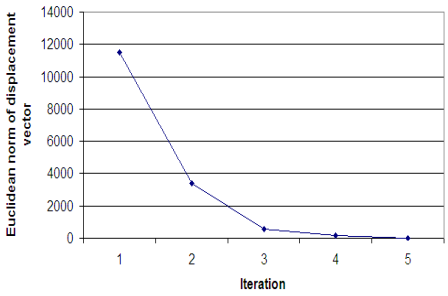

Fig. 3.8: Convergence history of GMRES solver solving non-linear case with quadratic potentials without template.

here GMRES solver rather than PCG solver, as our experiments indicate faster convergence .

The convergence history for the simulation with the template is shown in Figure 3.7. The vertical axis denotes absolute error with respect to Eucledean norm of the displacement vector. Total computational time is 167 seconds. The results of the simulation seem to be similar to those obtained with the linear model, which can be explained by small displacements occuring in that case.

However, the results of non-linear simulation for the case without template are improved. There is a similar shrinkage of the feature as in the linear model results, but there is no twisting of the feature. We conclude that the twist is associated with the linear model.

The convergence history for the simulation without template is shown in Figure 3.8. Total time is 218 seconds.

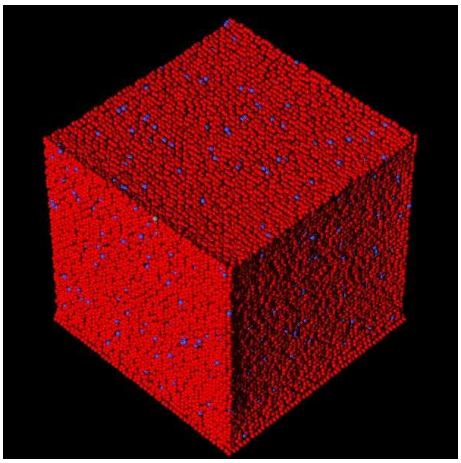

Fig. 3.9: Deformation of the feature inside the template provided by the non-linear model with quadratic potentials.

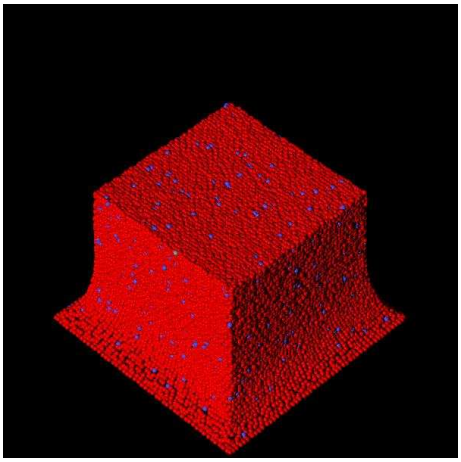

Fig. 3.10: Deformation of the feature outside the template provided by the non-linear model with quadratic potentials.

Non-linear mixed model with both quadratic and Lennard-Jones potentials, allowing for large displacements

Finally, we have implemented the non-linear model, allowing for mixing quadratic spring potentials for horizontal and vertical bounds, with Lennard-Jones potentials for cross-diagonal bounds. We have started the simulation outside the template from initial configuration, presented in Figure 3.4, like for all previously discussed cases. However, we have discovered problems with convergence of both GMRES and PCG solvers with Newton-Raphson loop.

We have performed the following experiment:

(1) Take the initial grid with parameters of quadratic potentials.
(2) Perform computations of non-linear model with quadratic potentials only,

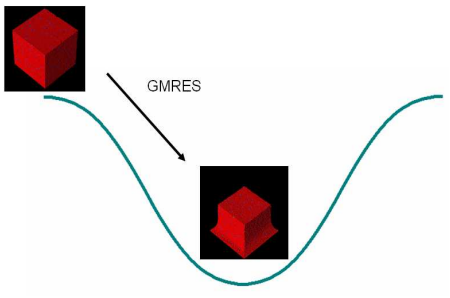

Fig. 3.11: Energy space for the non-linear model with quadratic potentials.

allowing for large displacements.

(3) Keep resulting configuration of the grid, but replace parameters of potentials into mixed quadratic and Lennard-Jones set.

(4) Run computations of non-linear mixed model with both quadratic and Lennard-Jones potentials

In other words, we have started mixed model computations from results of the previous model. The GMRES solver stops immediately displaying very small error, see Figure 3.13.

From that experiment the following conclusions imply:

- The energy space of the non-linear model with quadratic potentials only contains local energy of minimum close to the initial configuration of the feature, as presented in Figure 3.11. Iterative solvers find only local minimum of energy in energy space of the model. We conclude that in the energy space of the non-linear mixed model there are some local minimum of energy close to initial configuration, but those local minimums are only some artefacts of the model. The proper minimum in the mixed model energy space is located at the same place as minimum of energy in the non-linear spring model available from initial configuration. Thus, when we start computations from results of the non-linear spring model, we immediately obtain minimum of energy in the mixed model sense, as illustrated in Figure 3.12.
- There is no need for use of the mixed model, since mixed model results are similar to the non-linear spring model results.

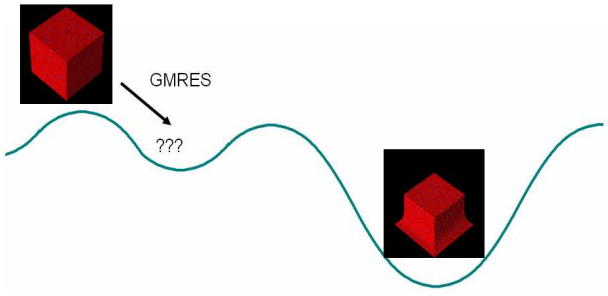

Fig. 3.12: Energy space for the mixed model with both quadratic and Lennard-Jones potentials..

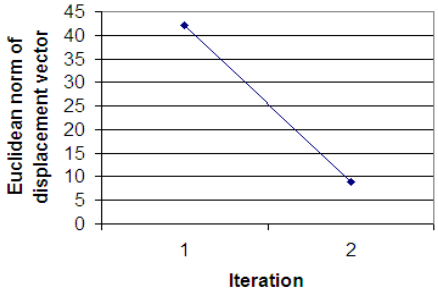

Fig. 3.13: Convergence history of GMRES solver solving non-linear case with mixed quadratic and Lennard-Jones potentials, with initial configuration provided by results of non-linear model with quadratic potentials.

3.3 Numerical analysis of the feature using a continuous linear elasticity model

In this section, we model the feature released from the template using linear elasticity.

The bulk properties of the feature are described by the following constitutive relations

$$\sigma_{ij} = 2\mu\varepsilon_{ij} + \lambda\delta_{ij}\varepsilon_{kk} - \alpha\delta_{ij}(3\lambda + 2\mu)(T - T_0)$$

Here α stands for the thermal expansion coefficent (CTE), T and T_0 are the current and reference temperatures and $\Delta T = (T - T_0)$ represents temperature gradient, μ and λ are the Lame coefficients which, in terms of the Young modulus E and Poisson ratio ν are given by

$$\mu = \frac{E}{2(1+\nu)} \qquad \lambda = \frac{\nu E}{1+\nu}$$

where

$$3\lambda + 2\mu = \frac{E}{1-2\nu}$$

The model is then specified by providing values of four parameters E, ν, ΔT and α. Following measurements presented in [1], [2], [3] we define Young modulus for the feature equal to $E = 1$ GPa, Poisson ratio $\nu = 0.3$, and thermal expansion coefficient as a 10 % volumetric shrinkage of the edge barier for the temperature gradient $\Delta T = 1^o K$ as $\alpha = \frac{\Delta V}{V \Delta T} = -0.1$.

We have performed finite element of the feature without template, assuming that the volumetric shrinkage is enforced by the thermal expansion coefficient involved in the constitutive equations within linear elasticity model.

The cube-shaped feature with all dimensions equal to 51×5.34 nm, fixed at the base, has been deformed in similar way as in the molecular statics computations, which is presented in figures *3.14, 3.15* and *3.16*.

Figures *3.14* and *3.15* presents symmetric displacements in x and y axis direction. The shrinkage of the feature is equal to 14 units, which is less than three times the distance between two consecutive particles in the intial configuration.

The z-displacement is equal to about 4 distances between particles in the initial grid configuration, as it is presented in Figure *3.16*.

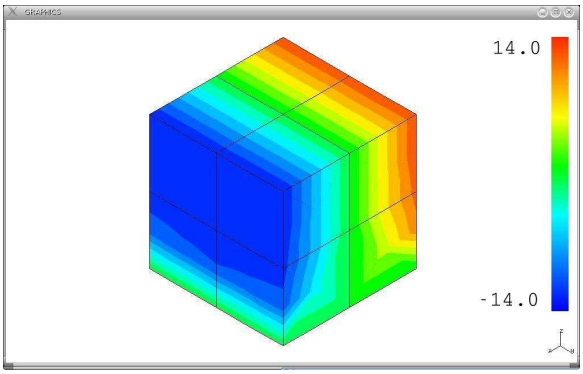

Fig. 3.14: Displacements of the feature in x axis direction.

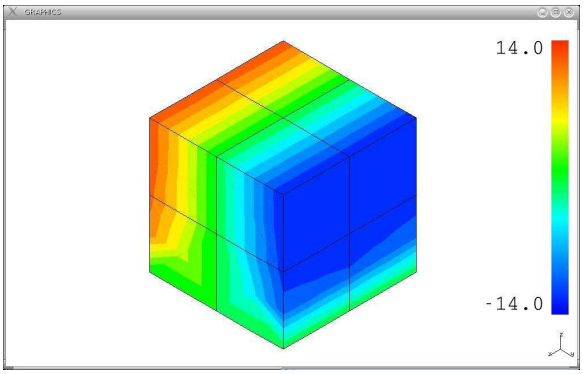

Fig. 3.15: Displacements of the feature in y axis direction.

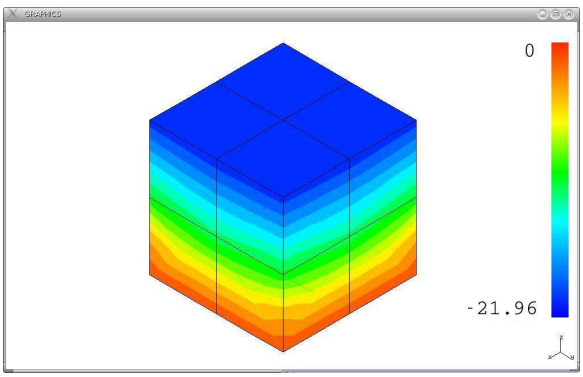

Fig. 3.16: Displacements of the feature in z axis direction.

4 Concluding Remarks

We have introduced three molecular statics models,

- Linear model assuming small deformations and spring potential functions.
- Non-linear model allowing for large deformation with spring potential functions.
- Non-linear model allowing for large deformations with Lennard-Jones potential functions.

We performed molecular statics simulations for linear model, non-linear quadratic potential model and mixed quadratic and Lennard-Jones potential model, for both the feature inside and outside the template.

From these experiments our concluding remarks are

- The results of the linear molecular statics model without the template show shrinkage of the feature with unexpected rotation of the whole feature. This is the consequence of the assumption of small displacement, which is not fullfilled in reality.
- The non-linear model with quadratic potentials results in the shrinkage of the feature without unexpected rotation. Most of the shrinkage occurs after the template is removed.
- The mixed model provides results similar to that of the nonlinear spring model.

We compared the molecular statics simulation of the feature outside the template with Finite Element Method computations where the shrinkage of the feature is enforced by the thermal expansion coefficient (CTE). The FEM results show smaler deformation than the molecular statics results. This may be the result of the coarse mesh used for the FEM simulation or improper estimation of the FEM model parameters. There is no experimental validation of the Poisson ratio used.

Acknowledgment
The first author was supported by the ICES Postdoctoral Fellowship Program. The support of this work, under Semiconductor Research Corporation Grant No. 2003-MJ-1082, is gratefully acknowledged.

References

[1] S. C. Johnson, "Step and Flash Imprint Lithography: Materials and Process Development" *Ph.D. Dissertation*, The University of Texas at Austin, 2005, pp.75-92.

[2] M. Colburn, I. Suez, B. J. Choi, M. Meissl, T. Bailey, S.V. Sreenivasan, J. G. Ekerdt, C. G. Willson, "Characterization and modeling of volumetric and mechanical properties for step and flash imprint lithography photopolymers" *J. Vac. Sci. Technol. B.*, 19(6), Nov/Dec 2001, pp.2685-2689.

[3] T. Bailey, B. Smith, B.J. Choi, M. Colburn, M. Meissl, S.V. Sreenivasan, J. G. Ekerdt, C. G. Willson, "Step and flash imprint lithography: Defect analysis" *J. Vac. Sci. Technol. B.*, 19(6), Nov/Dec 2001, pp.2806-2810.

[4] N.M. Putintsev, D.N. Putintsev "Method for Determining the Parameters of the Lennard-Jones Potential" *Deklady Physical Chemistry*, Vol.399, Part I, 2004, pp.278-282.

[5] T.C. Bailey, M.E. Colburn, B.J. Choi, A. Grot, J.G. Ekerdt, S.V. Sreenivasan, C.G. Willson, "Step and Flash Imprint Lithography: A Low-Pressure, Room Temperature Nanoimprint Patterning Process", in *Alternative Lithography. Unleashing the Potentials of Nanotechnology*, C. Sotomayor Torres, Editor. 2002, Elsevier.

[6] R. L.Burns, S. C.Johnson, G. M. Schmid, E. K. Kim, M. D. Dickey, J. Meiring, S. D. Burns, N. A. Stacey, C. G. Willson, "Mesoscale modeling for SFIL simulating polymerization kinetics and densification", Proc. SPIE, 5374, 348-360 (2004).

[7] SLATEC Common Mathematical Library http://www.netlib.org/slatec